Interplay of local moment and itinerant magnetism in cobalt-based Heusler ferromagnets: Co_{2}TiSi, Co_{2}MnSi and Co_{2}FeSi

Guanhua Qin, Wei Ren, and David J. Singh

Interplay of local moment and itinerant magnetism in cobalt-based Heusler ferromagnets: Co_2TiSi, Co_2MnSi and Co_2FeSi

Guanhua Qin,[1, 2, 3] Wei Ren,[1, 3, *] and David J. Singh[2, 4, †]

[1]*State Key Laboratory of Advanced Special Steel,*
Shanghai Key Laboratory of Advanced Ferrometallurgy and Physics,
Department, Shanghai University, Shanghai 200444, China
[2]*Department of Physics and Astronomy, University of Missouri, Columbia, MO 65211-7010, USA*
[3]*Shanghai Key Laboratory of High Temperature Superconductors,*
MGI and ICQMS, Shanghai University, Shanghai 200444, China
[4]*Department of Chemistry, University of Missouri, Columbia, MO 65211, USA*
(Dated: January 6, 2020)

Heusler ferromagnets based on Co are important materials for spintronics. This is due to the exceptional combinations of high Curie temperature and strong spin polarization, including half-metallicity, found in some of these. We investigate the full Heusler compounds, Co_2TiSi, Co_2MnSi and Co_2FeSi using first principles calculations. Co_2TiSi and Co_2MnSi are half-metals, while Co_2FeSi is not. The trends in the Curie temperatures are reproduced by the calculated spin wave dispersions. Remarkably, Co_2TiSi is a very itinerant magnet but Co_2FeSi and Co_2MnSi show local moment behavior regarding the Fe and Mn, while retaining the itinerancy of the Co magnetism. These materials can therefore be described as itinerant systems with embedded local moment atoms. This provides an explanation for their exceptional behavior. Our results do not support the half-metallic character proposed for Co_2FeSi. but they are consistent with a higher Curie temperature relative to the Mn compound. The density of states and transport spin polarizations Co_2FeSi have opposite signs. Importantly, although there is a large minority spin density of states at the Fermi level, leading to a low density of states spin polarization, we find a very strong transport spin polarization in Co_2FeSi. This, combined with the large moment, cubic structure and high Curie temperature supports the further investigation of Co_2FeSi for spintronic applications that make use of the transport spin polarization.

I. INTRODUCTION

Magnetic materials applicable to spintronics is a topic of strong interest. Cobalt and cobalt-based intermetallics are important magnetic materials, and are useful in technologies. This includes elemental cobalt, which is a high temperature ferromagnet with substantially itinerant character, Sm-Co hard magnets, such as $SmCo_5$, and Sm_2Co_{17},[1] as well as compounds showing weakly magnetic character as in pnictide superconductor related alloys ($BaFe_{2-x}Co_xAs_2$ and $BaCo_2As_2$).[2] The full Heusler ferromagnets, Co_2TiSi, Co_2MnSi and Co_2FeSi are remarkable from this perspective. These materials have been extensively investigated as potential half-metals,[3–17] and furthermore Co_2MnSi and Co_2FeSi show remarkably high Curie temperatures, T_C. In the case of Co_2FeSi, the reported Curie temperature is as high as 1100 K.[3,4] This suggests use in spintronic applications. However, as discussed below, the properties of Co_2FeSi in particular have been controversial, with the material having different reported Curie temperatures and being reported as half-metallic, ideal for spintronics, or not.

The high Curie temperature of Co_2FeSi has been discussed in literature in terms of a generalized Slater-Pauling rule in which the magnetic moment is understood in terms of electron count and T_C depends linearly on the magnetic moment.[18] Estimates of the Curie temperature based on spin-wave dispersions from spin spiral calculations support this high Curie temperature.[19]

However, there are also literature reports of lower Curie temperatures, $T_C \sim$ 980 K, and lower magnetizations in Co_2FeSi.[20,21] Co_2TiSi, which contains non-magnetic Ti, has T_C=380 K, while Co_2MnSi has T_C=985 K.[20,22–24]

The present paper examines these issues from the point of view of density functional calculations and provides a view of these materials as having a high Curie temperature and other magnetic properties controlled by the interplay of local moments associated with Fe and Mn that are embedded in an itinerant ferromagnetic background associated with the Co, as exemplified by Co_2TiSi. We also find that while Co_2FeSi is not half-metallic and is not close to being half-metallic from a density of states point of view, it does have a high transport spin polarization. This may enable some types of spintronic devices based on it, while at the same time making it unsuitable for other devices that depend on tunneling.

II. METHODS

The results reported here were obtained within density functional theory (DFT) using the Perdew-Burke-Ernzerhof generalized gradient approximation (PBE GGA),[25] except as noted. The calculations were done using the general potential linearized augmented planewave method,[26] as implemented in the WIEN2k and ELK codes.[27,28] We checked these two codes for consistency and find no significant differences for these materials.

The reported calculations are done at the experimental lattice parameters of 5.733 Å, for Co$_2$TiSi, 5.645 Å, for Co$_2$MnSi and 5.640 Å, for Co$_2$FeSi. The relaxed lattice parameters are very similar to these, specifically, 5,747 Å, 5.626 Å, and 5.632 Å, for Co$_2$TiSi, Co$_2$MnSi and Co$_2$FeSi, respectively. The close agreement of the lattice parameters supports the validity of the method used.

We note that there are prior calculations, based on the DFT+U methodology.[29] In those calculations it was found that adding U could lead to half-metallic ferromagnetism in Co$_2$FeSi for a certain range of the effective Hubbard interaction, U_{eff} in the range between 2 eV and 5 eV, but that values of U_{eff} of 2 eV or higher then leads to destruction of the experimentally observed half-metallic state in Co$_2$MnSi. Furthermore, as discussed below, the Co in these materials behaves very much as an itinerant system, similar to elemental Co. It has been shown that the use of DFT+U for such itinerant transition metals, including Fe and Co, leads to results in extremely poor agreement with experiment, even if first principles derived linear response values of U_{eff} are employed.[30,31] In fact PBE provides a much better description than higher level methods such as hybrid functionals, for these materials.[31] This is not to say that DFT+U is inferior to standard DFT for localized systems, such as many transition metal oxides.

Very recently, Nawa and Miura have proposed a mixed scheme where they apply DFT+U only to some transition element sites, particularly Fe and Mn in full-Heusler materials.[32] However, in bcc Fe, which shows more local moment behavior than Co,[33,34] similar to the Fe in the full-Heuslers, DFT+U calculations yield very poor agreement with experiment.[31] Furthermore, it might be expected from the fact that Co is to the right of Fe and Mn in the periodic table that Co should have larger or at least similar U to Fe and Mn. This is the case according to reported constrained density functional theory calculations of U for Co$_2$MnSi and Co$_2$FeSi.[35] It is not clear at this time if the mixed approach yields results in better accord with experiment for full-Heusler compounds. It is also noteworthy that GW calculations have been reported for Co$_2$FeSi that find good agreement with reported spectroscopic measurements similar to standard Kohn-Sham approaches but with an enhancement of the magnetization.[8]

Spin excitations were calculated within the framework of time dependent density functional theory (TDDFT), using the ELK code. Within TDDFT the magnon dispersions can be obtained from the transverse response function $\chi^+(\mathbf{q},\omega)$. This is determined by a Dyson-like[36] equation,[37–39]

$$\chi = \chi_0 + \chi_0(1 + f_{xc})\chi, \tag{1}$$

where χ is the physical (enhanced) susceptibility of the system, and f_{xc} is the exchange-correlation kernel, which is a functional derivative of the exchange-correlation potential. In this equation, χ_0 is the bare Kohn-Sham

TABLE I. Basic magnetic properties of the three compounds. All quantities are per formula unit. The magnetic energy, E_{mag}, is the energy difference between the non-spin-polarized and ferromagnetic solutions. $N(E_F)$ is the total electronic density of states at the Fermi level for both spins. M_{Co} and M_B are the spin moments in the Co and B (Ti, Mn or Fe) LAPW spheres and are given per atom. Note that they do not add to the total magnetization due to small Si and interstitial contributions.

	M_{spin} (μ_B)	M_{Co} (μ_B)	M_B (μ_B)	E_{mag} (eV)	$N(E_F)$ (eV^{-1})
Co$_2$TiSi	2.00	1.02	0.00	0.19	0.97
Co$_2$MnSi	5.00	1.06	3.00	1.59	0.77
Co$_2$FeSi	5.52	1.38	2.84	1.36	3.32

susceptibility. Here we used the adiabatic local density approximation (ALDA) for f_{xc}. The zone integration for these response calculations was done using a uniform 20×20×20 $\mathbf{k}$-point mesh in the Brillouin zone.

III. RESULTS AND DISCUSSION

We begin with the electronic structures. Co$_2$TiSi and Co$_2$MnSi are found to be half-metals with integer spin moments of 2 μ_B/f.u. and 5 μ_B/f.u., respectively. This is in accord with experiment and prior theoretical work.[6,19,22,23] We do not obtain a half-metallic state for Co$_2$FeSi. The calculated spin moment is 5.52 μ_B/f.u. Basic magnetic properties of the three compounds are summarized in Table I. The individual moments, as given by the integrated spin moments in the corresponding LAPW spheres, are also shown. As seen, the Co spin moments for half-metallic Co$_2$TiSi and Co$_2$MnSi are similar, while the value for Co$_2$FeSi is larger, indicating a difference in electronic structure.

The band structures of ferromagnetic Co$_2$TiSi, Co$_2$MnSi and Co$_2$FeSi are shown in Fig. 1, along with the corresponding electronic densities of states. These electronic structures are similar to those reported previously.[7,19,22,23,40] Both Co$_2$TiSi and Co$_2$MnSi show gaps in the minority spin leading to half-metallic behavior, while Co$_2$FeSi does not have such a gap and is not a half-metal according to these calculations. This is also evident from the non-integer spin magnetization, as mentioned above. Importantly, there is a dispersive minority spin band that dips below the Fermi level, E_F, at the X point in Co$_2$FeSi. This extends to ∼-0.6 eV, relative to E_F, and almost touches the next lower minority band at X. This makes it impossible for small changes to lead to half-metallic behavior.

Thus transport in both spin channels is expected for Co$_2$FeSi. However, we find a very strong spin polarization for transport even though the density of states in the minority spin is substantial. This means that even though it is not a half-metal according to our calcu-
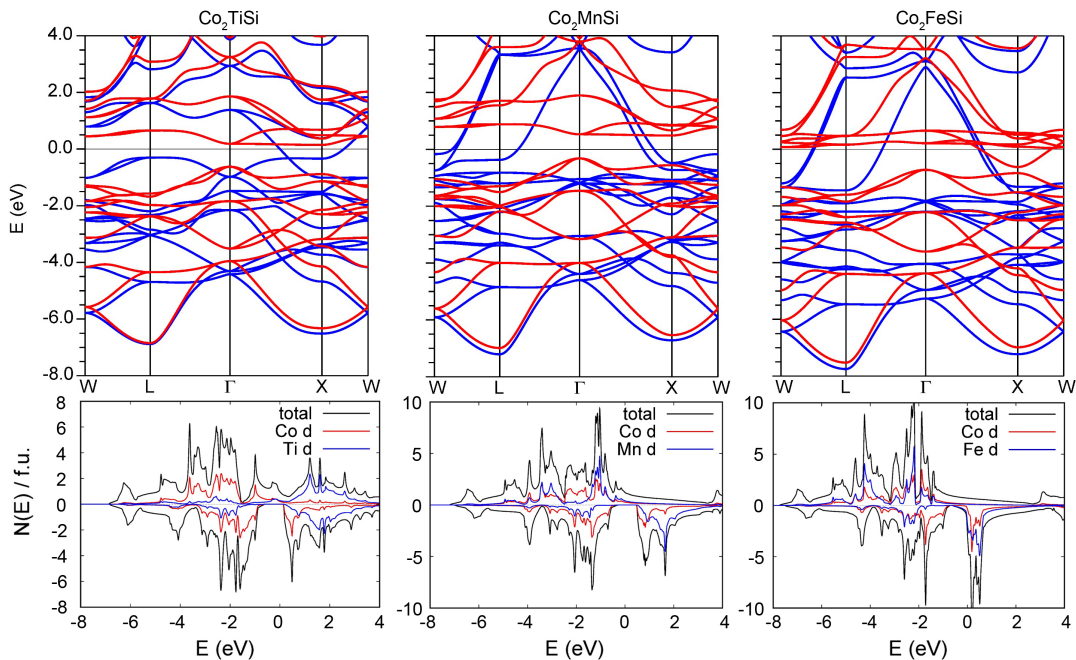
FIG. 1. Calculated band structures of the Co$_2B$Si compounds (top). Majority spin bands are shown in blue and minority spin in red. Note that all three compounds have very dispersive majority spin bands (blue) crossing the Fermi level, and much less dispersive minority spin bands (red) just above the Fermi level, E_F. Electronic densities of states are in the bottom panels. Majority spin is shown as positive and minority spin is negative. Projections are of d-character in the corresponding LAPW spheres of radii 2.3 Bohr and 1.8 Bohr, for the metal and Si atoms, respectively.

lations, Co$_2$FeSi may nonetheless be a useful material for spintronics especially considering its cubic structure and high Curie temperature. Furthermore the density of states and transport spin polarization are opposite. This is an interesting case because experiments in between the diffusive and tunnelling regimes may then measure particularly low spin polarization, while more ideal devices in the diffusive regime may be able to exploit the high transport spin polarization.

This rather unusual situation where one has high transport spin polarization and low opposite sign density of states spin polarization is due to the specific band structure of the material. The majority and minority spin Fermi surfaces responsible for this are shown in Fig. 2. The majority spin shows two large sheets of Fermi surface, with a nearly spherical shape. The minority spin shows two sheets, These are one flattened sheet at the X-point of the Brillouin zone and a small section at the K point (the center of the connection between two W points). As seen in Fig. 1, the minority spin Fermi surface originates in much less dispersive bands than the majority spin Fermi surface. This is also evident in the density of states of Fig. 1. The Fermi level occurs in a flat region of density of states for the majority spin, characteristic of wide bands, while the minority spin is at the onset of a relatively narrow peak in the density of states derived from Co d and Fe d states.

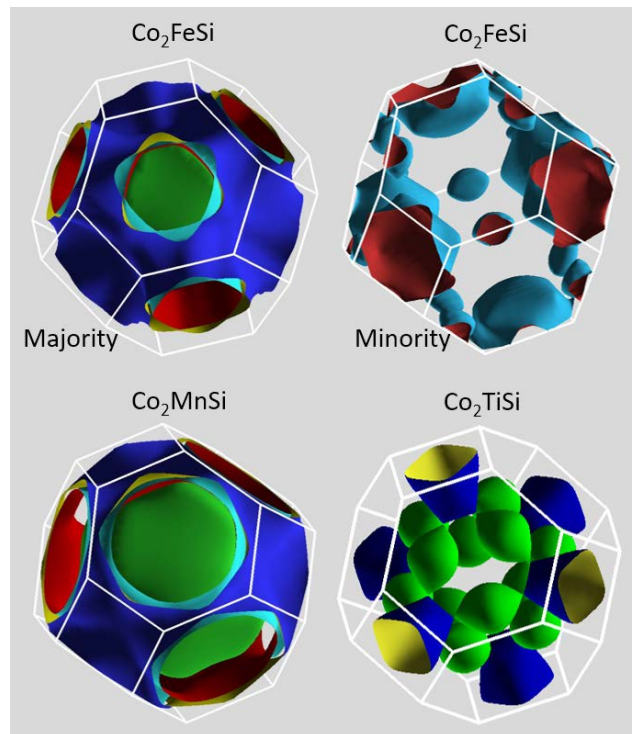The spin polarization for quantity f is defined as

FIG. 2. Majority (top, left) and minority spin (top, right) Fermi surface of Co$_2$FeSi. along with the majority spin Fermi surfaces of half-metallic Co$_2$MnSi (bottom, left) and Co$_2$TiSi (bottom, right).

TABLE II. Electronic properties at the Fermi energy. $N(E_F)$ is given in eV^{-1} per formula unit and σ/τ is given in 10^{21} $(\Omega\mathrm{ms})^{-1}$.

	$N(E_F)_\uparrow$	$N(E_F)_\downarrow$	P_D	$(\sigma/\tau)_\uparrow$	$(\sigma/\tau)_\downarrow$	P_σ
Co$_2$TiSi	0.97	0.00	1.00	0.31	0.00	1.00
Co$_2$MnSi	0.77	0.00	1.00	0.82	0.00	1.00
Co$_2$FeSi	0.71	2.61	-0.57	1.46	0.10	0.87

$$P_f = \frac{f_\uparrow - f_\downarrow}{f_\uparrow + f_\downarrow}. \tag{2}$$

Here f can be the conductivity, σ, to produce the transport spin polarization, P_σ, the density of states, $D=N(E_F)$, for the density of states spin polarization, P_D, or other quantities.

We did transport calculations based on the calculated electronic structure using the BoltzTraP code.[41] This code yields the transport integral for the conductivity, σ modulo an undetermined scattering time, τ. The value quoted is from calculations at 50 K, but there is very little temperature dependence. The value of the transport spin polarization at 300 K is only 2% smaller. The obtained value of σ/τ is proportional to the product of electronic density of states $N(E_F)$ and average Fermi velocity, $<v_F^2>$ at low temperature. In a parabolic band model with fixed number of carriers the resulting σ/τ is inversely proportional to the effective mass, m^*, reflecting the fact that although they lead to high density of states flat bands are unfavorable for transport.

In any case, σ/τ is sufficient to calculate the transport spin polarization with the assumption that the scattering time is the same for the two spin channels. This assumption has been applied to complex magnetic systems, for example, SrRuO$_3$, where a reasonable description of experimental data is found. This includes predictions, as in SrRuO$_3$, where an unexpected transport spin polarization opposite to the magnetization was predicted and then found experimentally.[42–44] In general, the scattering mechanisms can have spin dependence and in general this depends on sample details. Nonetheless in a high spin polarization material such as we find for Co$_2$FeSi this is unlikely to lower the spin polarization strongly, and furthermore in Co$_2$FeSi the density of states is higher in the minority spin channel, which would suggest if anything a lower τ for that spin channel with an enhancement of the already high transport spin polarization.

As seen, the density of states spin polarization of Co$_2$FeSi is modest and negative. However, the transport spin polarization is very high. Additionally, it is interesting to observe that it is positive, in other words that it has opposite sign to the density of states spin polarization. Returning to the electronic structure, it may be noted that the minority spin gap in the parent compound, Co$_2$TiSi, is between groups of Co d derived bands with relatively high density of states reflecting rel-
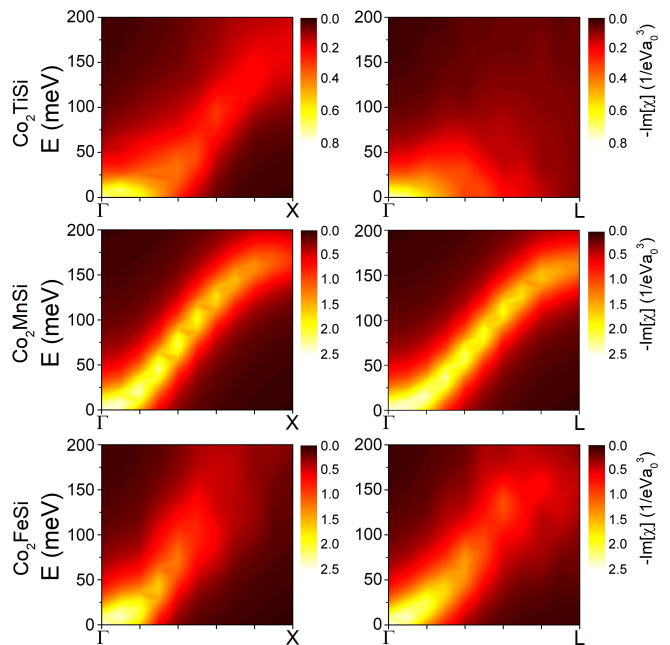

FIG. 3. Spin excitations plotted as the imaginary part of the susceptibility from TDDFT calculations. The left panels show the Γ-X direction, while the right panels show Γ-L.

atively flat dispersion (note here we refer to Co$_2$TiSi as the parent, because Ti is non-magnetic and the other compounds have magnetic atoms on the Ti site). On the other hand, the Fermi level lies in a lower density of states region for the majority spin which has substantial non-transition metal (Si) character. The corresponding bands are considerably more dispersive as is evident in the band structure. In the cases of Co$_2$MnSi and Co$_2$FeSi the Fermi level lies above the d bands for majority spin, i.e. it is in a region of broad Si derived bands with little d character. This is similar to the band character of NiSi, which is an electrode material with a remarkably high conductivity.[45–47] On the other hand, the minority spin Fermi level lies in a region of d bands, in particular in a gap between d bands for Co$_2$MnSi and in the lower part of a d band peak Co$_2$FeSi.

Magnetic tunnel junctions have been fabricated using Co$_2$FeSi by Gersci and co-workers.[9] The magnetoresistance in this type of device is governed by the density of states spin-polarization, P_D,[48–50] although there is also a dependence on the nature of the interfaces and tunneling probabilities that may depend on details of the band structure. This is discussed in detail in Ref. 50. In any case, Gersci and co-workers obtained a value of the spin polarization $P=0.50$ from these measurements. This is close in magnitude to the value of $P_D=-0.57$ from our band calculations. One may note that P occurs in products in the Julliere formula,[48–50]
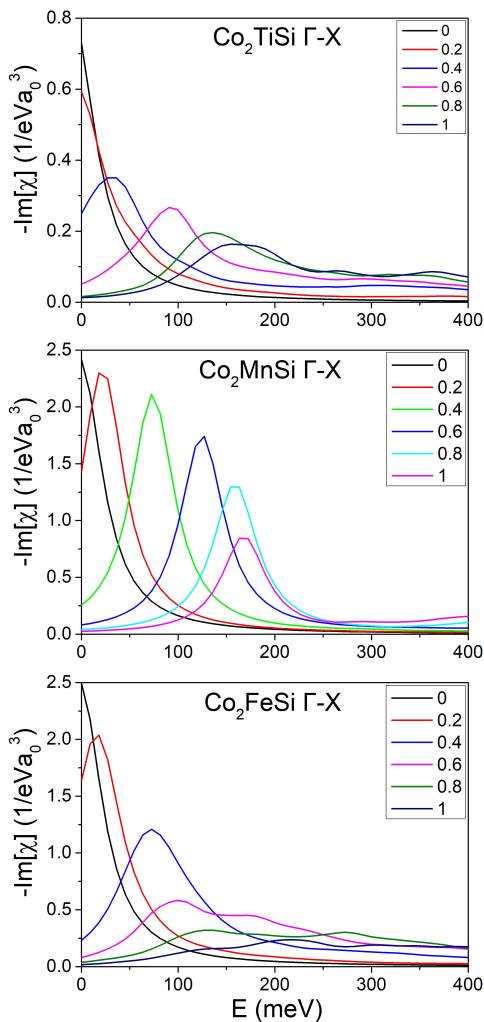
$$TMR = 2P_1P_2/(1 - P_1P_2), \tag{3}$$

FIG. 4. Energy dependent imaginary susceptibilities for different crystal momenta, along Γ-X, where 0 corresponds to Γ and 1 corresponds to X.
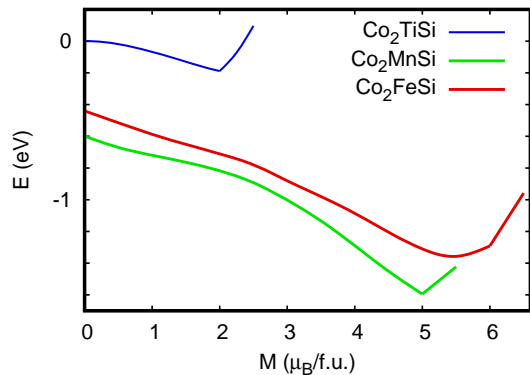

FIG. 5. Fixed spin moment energy as a function of magnetization. The energy zero is taken as the energy of a non-spin-polarized calculation. Note that for Co_2MnSi and Co_2FeSi the zero moment solution has opposite Co and Mn or Fe moments, and an energy below the non-spin polarized solution. Energies and magnetizations are per formula unit.

where the tunneling magnetoresistance TMR is controlled by the spin polarization of the density of states polarization at the Fermi level of the two materials, P_1 and P_2, so that the absolute sign may be difficult to determine.

Point contact Andreev reflection (PCAR) measurements were reported on different samples.[9,12] In this method a superconducting tip is brought into contact with the sample and the Andreev reflection is measured using the dependence of the conductivity on bias voltage.[51–53] These studies yielded PCAR polarizations in the range 48% to 59%. The PCAR spin polarization is equal to the transport spin polarization in the case where there is strong scattering in the sample, i.e. in the diffusive limit. However, these measurements require a junction with a superconducting material, and therefore must be done at low temperature, where the transport may be intermediate between diffusive and ballistic. In the ballistic regime the transport is governed by states weighted by the band velocity in the direction of transport, rather than the square of the band velocity. This introduces both geometry and sample dependence.[51–55] Nonetheless those measurements are indicative of sizable spin polarization, but are inconsistent with true half-metallic behavior.

We also did calculations including spin-orbit coupling to check whether orbital moments could explain the difference between the spin-magnetization and the reported low temperature magnetization as reported by Wurmehl and co-workers.[3,4] We find orbital moments parallel to the spin moments, as expected based on Hund's third rule for a more than half full shell. However, the values are m_{orb}=0.040 μ_B for Co and m_{orb}=0.067 μ_B for Fe, for a total orbital moment of 0.147 μ_B per formula unit. This is far too small to explain the discrepancy.

An interesting puzzle is then the high Curie temperature. This was explained using an itinerant Slater-Pauli relation. The explanation is based on half-metallicity and a linear connection between the magnetization and the Curie temperature.[18] However, we do not find half-metallicity and this is consistent with other recent calculations and several experiments. Within this picture, Co_2FeSi might be expected to have significantly lower Curie temperatures if the magnetization were lower than the half-metallic value. On the other hand, the strong experimental evidence of finite spin polarization is difficult to reconcile with a half-metallic state and therefore with a spin magnetization of 6 μ_B per formula unit. We therefore compare the spin excitations of Co_2MnSi and Co_2FeSi, using density functional calculations. These calculations do not produce a half-metallic state and therefore address the question of whether the high Curie temperature is linked to half-metallicity. The result of these TDDFT calculations is shown in Fig. 3. Cuts at different $\mathbf{k}$-points along Γ-X are shown in Fig. 4. As seen, the spin excitations of Co_2TiSi become incoherent away from the zone center. This is a consequence of

the itinerant nature of the material and especially transitions to minority spin states just above the Fermi level as seen in the band structure. It should also be noted from Fig. 4 that there are additional small broad peaks in the imaginary susceptibility at energies above the lowest magnon branch, especially towards the zone boundary in Co_2TiSi and Co_2FeSi. In a local moment Heisenberg picture, with three magnetic atoms per unit cell, three magnon branches may be expected, while with two magnetic atoms per cell, as in Co_2TiSi, two branches may be expected. In itinerant materials, the spectral function reflects electronic excitations, and can have different numbers of peaks, often with considerable damping. The present materials show complex behavior with low amplitude broad peaks at higher energy, reflecting the itinerant nature of the magnetism.

One notes that the energy scales for Co_2MnSi and Co_2FeSi are similar, but that Co_2FeSi has a higher stiffness near Γ. A fit of the spin wave dispersion to a quadratic form appropriate for a ferromagnet yields a coefficient $D=197$ meV $Å^2$ for Co_2MnSi and $D=222$ meV $Å^2$ for Co_2FeSi. This is consistent with a $\sim15\%$ higher Curie temperature in the Fe compound, although it is not a half-metal. A similar fit for Co_2TiSi yields a much smaller $D=86$ meV $Å^2$, consistent with its much lower Curie temperature.

Magnetic materials are often classified according to the extent to which they are itinerant or local moment in nature.[56–58] In the local moment limit, stable moments are present on the ions due to intra-atomic interactions. These are subject to inter-site interactions that provide the magnetism through ordering of the moments. Local moment magnets can often be described by the Heisenberg or related spin models. The opposite, itinerant limit, is exemplified by materials such as $ZrZn_2$, and to a lesser extents elemental Ni and Co.[57] In this limit, there are not stable moments, but instead ordering arises from conduction electrons, and in fact magnetic states may not even exist for some ordering patterns. This is seen for example from merging of spin-wave excitations seen by neutron scattering into a Stoner continuum at high wavevectors.[59] This can lead to very high ordering temperatures, such as the very high Neel temperature found in $SrTcO_3$.[60] Both of these types of magnetism can be described by DFT calculations, as exemplified by work on $BaMn_2As_2$, Y_2Ni_7 and other materials.[61–64] The Slater-Pauling curve that was used to understand the Curie temperatures of Heusler compounds is based on an itinerant framework. In order to address the issue of the magnetic nature of these compounds we did calculations including fixed spin moment calculations.[65,66]

We begin with Co_2TiSi. This may be regarded as the parent compound of Co_2MnSi and Co_2FeSi, where the magnetic Mn or Fe atom is replaced by the magnetically inert element Ti. The connection between the three compounds is emphasized by the similar structures in the electronic densities of states for the Co sites (lower panels of Fig. 1), although the Fermi levels differ due to
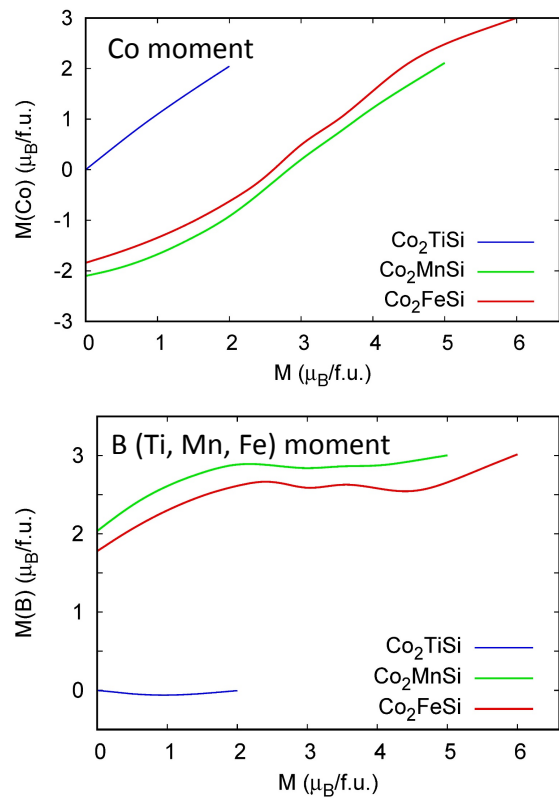

FIG. 6. Fixed spin moment moments as a function of the total moment per unit cell. The moments are per formula unit, i.e. the moment in the two Co atoms (upper panel) and in the B (Ti, Mn or Co) atom (lower panel).

the different electron counts. We attempted to stabilize an antiferromagnetic solution for Co_2TiSi in which the two Co atoms in the unit cell have opposite spin. We did this by performing self consistent calculations with various initial conditions, and also by performing fixed spin moment calculations with the total moment set to zero and opposite moments as the initial condition. The only solution that we were able to find was one in which the moments were zero. As mentioned the fact that moments are only stable for some arrangements means that this is not a local moment system, and is instead itinerant. This itinerant nature of Co_2TiSi is consistent with the conclusions of Barth and co-workers.[22,23]

However, in contrast to Co_2TiSi, fixed spin moment calculations for Co_2MnSi and Co_2FeSi with zero total moment do have spin polarized solutions. In particular with the total moment set to zero we find Mn and Fe moments opposite to the Co. This indicates stability of the Fe and Mn moments. The calculated energies as a function of spin magnetization for the three compounds are shown in Fig. 5. The corresponding moments in the transition element LAPW spheres (radius 2.3 Bohr) are shown in Fig. 6. As seen, the magnetic energy scales for Co_2MnSi and Co_2FeSi are much higher than that of Co_2TiSi. Also the minimum energies for Co_2TiSi and

Co_2MnSi are at integer spin magnetization, while that of Co_2FeSi is not, in accord with the self-consistent calculations.

The individual moments show that there is practically no polarization of Ti, as expected. Importantly, the Co moments behave very differently than the Fe and Mn moments. In particular, the constraint of the fixed spin moment is achieved almost entirely through variation of the Co moments, while the Mn and Fe moments are much stiffer. This means that the Fe and Mn atoms behave as if they have local moments, while the Co backbone is itinerant in nature.

Therefore, the magnetic behavior of Co_2MnSi and Co_2FeSi can be understood in terms of local Mn or Fe moments interacting with an itinerant electron system. Interestingly, this is similar to the well known spintronic material, (Ga,Mn)As, where itinerant holes mediate interactions between Mn local moments.[67] The difference in the present case is that here the itinerant background is already an ordered ferromagnet.

IV. SUMMARY AND CONCLUSIONS

We report a density functional study of the ferromagnetic cobalt-based Heusler silicides, in particular Co_2MnSi, Co_2FeSi and the parent compound Co_2TiSi. We find that Co_2FeSi is not half-metallic, similar to prior standard density functional studies. However, we find nonetheless that although not a half-metal, it has a very high transport spin polarization, and interestingly this is opposite to the density of states spin polarization. While this is not important for tunneling magnetoresistance devices, such as those used in read heads of hard disk technology, it is germane to other spintronic applications in-

volving spin polarized currents. We also find that the spin excitations from our calculations, which do not yield a half-metallic state for Co_2FeSi, are nonetheless consistent with the experimental observation of a higher T_C for Co_2FeSi than for Co_2MnSi. Fixed spin moment calculations imply that the magnetic ordering can be understood in terms of local moments on Mn or Fe interacting through an itinerant ferromagnetic background associated with the Co-Si framework of these compounds.

It is important to note that the chemistry and properties of Co_2FeSi are compatible with conventional electronics[68] and that transition metal silicides have been extensively used as electrode materials for Si devices.[45] Moreover Co_2FeSi has a cubic crystal structure. The lattice parameter is ∼4% larger than that of Si, and is a very close match to both Ge and GaAs. These facts along with the high Curie temperature and high transport spin polarization suggest further investigations of Co_2FeSi as a spintronic material. The results also suggest additional experiments to confirm the low temperature spin magnetization of well ordered Co_2FeSi.

ACKNOWLEDGMENTS

* renwei@shu.edu.cn

† singhdj@missouri.edu

1 O. Gutfleisch, J. Phys. D: Appl. Phys. **33**, 157 (2000).

2 A. S. Sefat, R. Jin, M. A. McGuire, B. C. Sales, D. J. Singh, and D. Mandrus, Phys. Rev. Lett. **101**, 117004 (2008).

3 S. Wurmehl, G. H. Fecher, H. C. Kandpal, V. Ksenofontov, C. Felser, H. J. Lin, and J. Morais, Phys. Rev. B **72**, 184434 (2005).

4 S. Wurmehl, G. H. Fecher, H. C. Kandpal, V. Ksenofontov, and C. Felser, Appl. Phys. Lett. **88**, 032503 (2006).

5 D. Comtesse, B. Geisler, P. Entel, P. Kratzer, and L. Szunyogh, Phys. Rev. B **89**, 094410 (2014).

6 M. Jourdan, J. Minar, J. Braun, A. Kronenberg, S. Chadov, B. Balke, A. Glskovskii, M. Kolbe, H. J. Elmers, G. Schonhense, H. Ebert, C. Felser, and M. Klaui, Nature Comm. **5**, 3974 (2014).

7 E. Sasioglu, L. M. Sandratskii, P. Bruno, and I. Galanakis, Phys. Rev. B **72**, 184415 (2005).

8 M. Meinert, C. Friedrich, G. Reiss, and S. Blugel, Phys. Rev. B **86**, 245115 (2012).

9 Z. Gersci, A. Rajanikanth, Y. K. Takahashi, K. Hono, M. Kikuchi, N. Tezuka, and K. Inomata, Appl. Phys. Lett. **89**, 082512 (2006).

10 K. Inomata, S. Okamura, A. Miyazaki, M. Kikuchi, N. Tezuka, M. Wojcik, and E. Jedryka, J. Phys. D: Appl. Phys. **39**, 816 (2006).

11 C. G. F. Blum, C. A. Jenkins, J. Barth, C. Felser, S. Wurmehl, G. Friemel, C. Hess, G. Behr, B. Buchner, A. Reller, S. Riegg, S. G. Ebbinghaus, T. Ellis, P. J. Jacobs, J. T. Kohlhepp, and H. J. M. Swagten, Appl. Phys. Lett. **95**, 161903 (2009).

12 L. Makinistian, M. M. Faiz, R. P. Panguluri, B. Balke, S. Wurmehl, C. Felser, E. A. Albanesi, A. G. Petukhov, and B. Nadgorny, Phys. Rev. B **87**, 220402(R) (2013).

13 Y. Takamura, T. Suzuki, Y. Fujino, and S. Nakagawa, J. Appl. Phys. **115**, 17C732 (2014).

14 M. Emmel, A. Alfonsov, D. Legut, A. Kehlberger, E. Vilanova, I. P. Krug, D. M. Gottlob, M. Belesi, B. Buchner, M. Klaui, P. M. Oppeneer, S. Wurmehl, H. J. Elmers, and G. Jakob, J. Magn. Magn. Mater. **368**, 364 (2014).

15 W. Zhu, D. Wu, B. Zhao, Z. Zhu, X. Yang, Z. Zhang, and

[15] Q. Y. Jin, Phys. Rev. Appl. **8**, 034012 (2017).

[16] W. Zhu, Z. Zhu, D. Li, G. Wu, L. Xi, Q. Y. Jin, and Z. Zhang, J. Magn. Magn. Mater. **479**, 179 (2019).

[17] T. Graf, C. Felser, and S. S. P. Parkin, Prog. Solid State Chem. **39**, 1 (2011).

[18] G. H. Fecher, H. C. Kandpal, S. Wurmehl, and C. Felser, J. Appl. Phys. **99**, 08J106 (2006).

[19] J. Kubler, G. H. Fecher, and C. Felser, Phys. Rev. B **76**, 024414 (2007).

[20] K. H. J. Buschow, P. G. van Engen, and R. Jongebreur, J. Magn. Magn. Mater. **38**, 1 (1983).

[21] V. Niculescu, T. J. Burch, K. Raj, and J. I. Budnick, J. Magn. Magn. Mater. **5**, 60 (1977).

[22] J. Barth, G. H. Fecher, B. Balke, T. Graf, A. Shkabko, A. Weidenkaff, P. Klaer, M. Kallmayer, H. J. Elmers, H. Yoshikawa, S. Ueda, K. Kobayashi, and C. Felser, Phil. Trans. Roy. Soc. A **369**, 3588 (2011).

[23] J. Barth, G. H. Fecher, B. Balke, S. Ouardi, T. Graf, C. Felser, A. Shkabko, A. Weidenkaff, P. Klaer, H. J. Elmers, H. Yoshikawa, S. Ueda, and K. Kobayashi, Phys. Rev. B **81**, 064404 (2010).

[24] P. J. Webster, J. Phys. Chem. Sol. **32**, 1221 (1971).

[25] J. P. Perdew, K. Burke, and M. Ernzerhof, Phys. Rev. Lett. **77**, 3865 (1996).

[26] D. J. Singh and L. Nordstrom, *Planewaves, Pseudopotentials, and the LAPW method*, 2nd *Ed.* (Springer, Berlin, 2006).

[27] P. Blaha, K. Schwarz, G. K. H. Madsen, D. Kvasnicka, and J. Luitz, WIEN2k, An augmented plane wave+local orbitals program for calculating crystal properties (2001).

[28] K. Dewhurst, Http://elk.sourceforge.net/.

[29] H. C. Kandpal, G. H. Fecher, C. Felser, and G. Schonhense, Phys. Rev. B **73**, 094422 (2006).

[30] M. Cococcioni and S. de Gironcoli, Phys. Rev. B **71**, 035105 (2005).

[31] Y. Fu and D. J. Singh, Phys. Rev. B **100**, 045126 (2019).

[32] K. Nawa and Y. Miura, RSC Adv. **9**, 30462 (2019).

[33] P. J. Brown, K. R. A. Ziebeck, J. Desportes, and D. Givord, J. Appl. Phys. **55**, 1881 (1984).

[34] H. A. Mook and J. W. Lynn, J. Appl. Phys. **57**, 3006 (1985).

[35] E. Sasioglu, I. Galanakis, C. Friedrich, and S. Blugel, Phys. Rev. B **88**, 134402 (2013).

[36] F. J. Dyson, Phys. Rev. **75**, 1736 (1949).

[37] E. K. U. Gross and W. Kohn, Phys. Rev. Lett. **55**, 2850 (1985).

[38] P. Buczek, A. Ernst, P. Bruno, and L. M. Sandratskii, Phys. Rev. Lett. **102**, 247206 (2009).

[39] N. Singh, P. Elliott, T. Nautiyal, J. K. Dewhurst, and S. Sharma, Phys. Rev. B **99**, 035151 (2019).

[40] V. Sharma, A. K. Solanki, and A. Kashyap, J. Magn. Magn. Mater. **322**, 2922 (2010).

[41] G. K. H. Madsen and D. J. Singh, Comput. Phys. Commun. **175**, 67 (2006).

[42] D. J. Singh, J. Appl. Phys. **79**, 4818 (1996).

[43] B. Nadgorny, M. S. Osofsky, D. J. Singh, G. T. Woods, R. J. Soulen, Jr., M. K. Lee, S. D. Bu, and C. B. Eom, Appl. Phys. Lett. **82**, 427 (2003).

[44] D. C. Worledge and T. H. Geballe, Phys. Rev. Lett. **85**, 5182 (2000).

[45] J. P. Gambino and E. G. Colgan, Mater. Chem. Phys. **52**, 99 (1998).

[46] A. Dahal, J. Gunasekera, L. Harringer, D. K. Singh, and D. J. Singh, J. Alloys Compds. **672**, 110 (2016).

[47] Y. Wu, J. Xiang, C. Yang, W. Lu, and C. M. Lieber, Nature (London) **430**, 61 (2004).

[48] M. Julliere, Phys. Lett. A **54**, 225 (1975).

[49] J. S. Moodera, L. R. Kinder, T. M. Wong, and R. Meservey, Phys. Rev. Lett. **74**, 3273 (1995).

[50] E. Y. Tsymbal, O. N. Mryasov, and P. R. LeClair, J. Phys.:Condens. Matter **15**, R109 (2003).

[51] M. J. M. de Jong and C. W. J. Beenakker, Phys. Rev. Lett. **74**, 1657 (1995).

[52] R. J. Soulen, Jr., J. M. Byers, M. S. Osofsky, B. Nadgorny, T. Ambrose, S. F. Cheng, P. R. Boussard, C. T. Tanaka, J. Nowak, J. S. Moodera, A. Barry, and J. M. D. Coey, Science **282**, 85 (1998).

[53] Y. Ji, G. J. Strijkers, F. Y. Yang, C. L. Chien, J. M. Byers, A. Anguelouch, G. Xiao, and A. Gupta, Phys. Rev. Lett. **86**, 5585 (2001).

[54] G. E. Blonder, M. Tinkham, and T. M. Klapwijk, Phys. Rev. B **25**, 4515 (1982).

[55] I. I. Mazin, A. A. Golubov, and B. Nadgorny, J. Appl. Phys. **89**, 7576 (2001).

[56] E. C. Stoner, Proc. R. Soc. Lond. Ser. A **169**, 339 (1939).

[57] T. Moriya and Y. Takahashi, Ann. Rev. Mater. Sci. **14**, 1 (1984).

[58] E. Svanidze, J. K. Wang, T. Besara, L. Liu, Q. Huang, T. Siegrist, B. Frandsen, J. W. Lynn, A. H. Nevidomskyy, M. B. Gamza, M. C. Aronson, Y. J. Uemura, and E. Morosan, Nature Comm. **6**, 7701 (2015).

[59] H. A. Mook and D. M. Paul, Phys. Rev. Lett. **54**, 227 (1985).

[60] E. E. Rodriguez, F. Poineau, A. Llobet, B. J. Kennedy, M. Avdeev, G. J. Thorogood, M. L. Carter, R. Seshadri, D. J. Singh, and A. K. Cheetham, Phys. Rev. Lett. **106**, 067201 (2011).

[61] J. An, A. S. Sefat, D. J. Singh, and M. H. Du, Phys. Rev. B **79**, 075120 (2009).

[62] C. J. Honer, M. J. Prosniewski, A. Putatunda, and D. J. Singh, J. Phys.: Condens. Matter **29**, 405501 (2017).

[63] D. J. Singh, Phys. Rev. B **92**, 174403 (2015).

[64] A. R. M. Iasir, T. Lombardi, Q. Lu, A. M. Mofrad, M. Vaninger, X. Zhang, and D. J. Singh, Cond-Mat , arXiv:1910.09923 (2019).

[65] K. Schwarz and P. Mohn, J. Phys. F: Metal Phys. **14**, L129 (1984).

[66] V. L. Moruzzi, P. M. Marcus, K. Schwarz, and P. Mohn, Phys. Rev. B **34**, 1784 (1986).

[67] F. Matsukura, H. Ohno, A. Shen, and Y. Sugawara, Phys. Rev. B **57**, R2037 (1998).

[68] Y. Takamura, R. Nakane, H. Munekata, and S. Sugahara, J. Appl. Phys. **103**, 07D719 (2008).